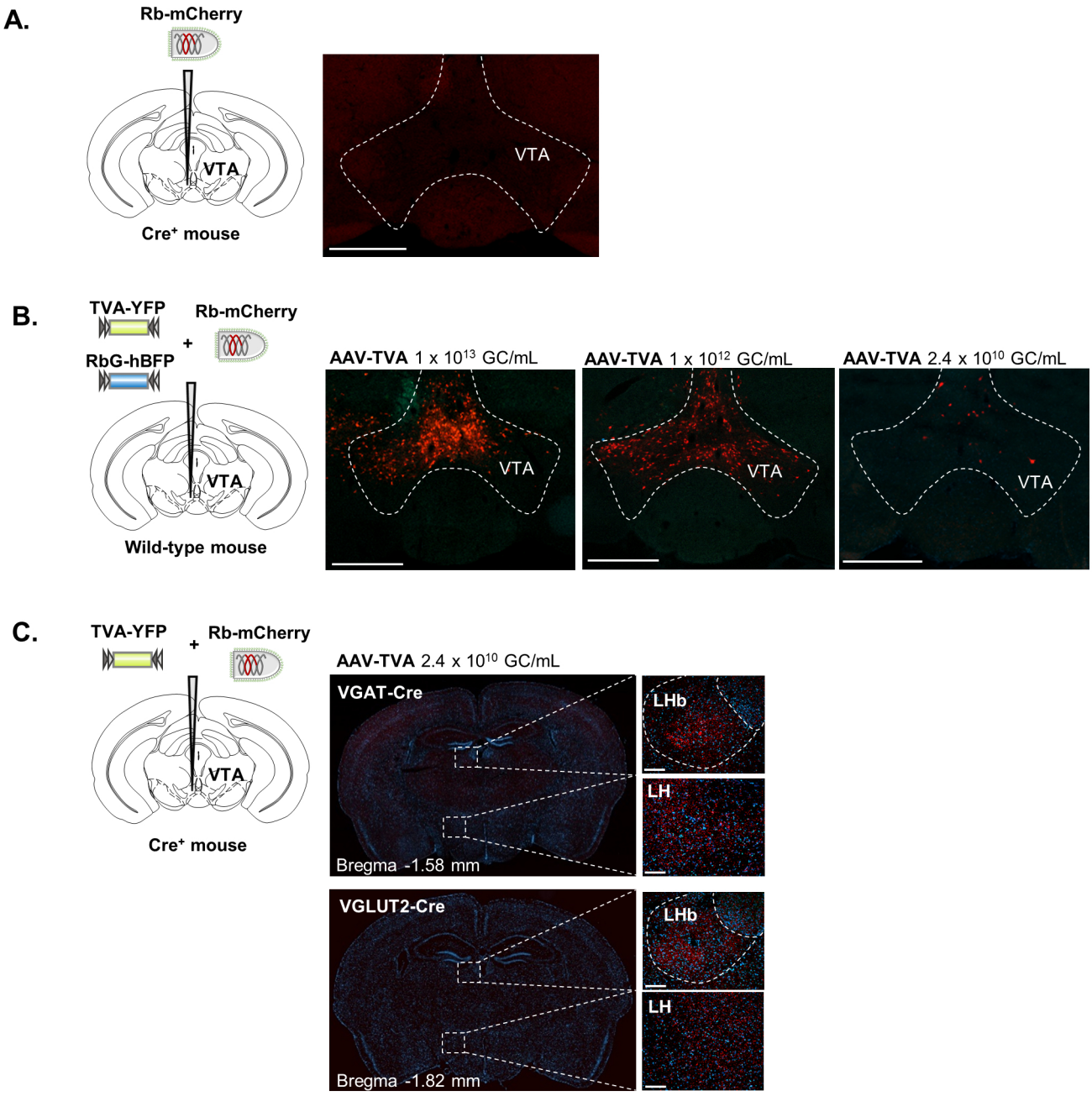

Figure S1, related to Figure 1. Controls demonstrating specificity of transynaptic tracing approach. A. No mCherry+ cells were detected either at the injection site or at distal sites following injection of EnvA-Rb-ΔG-mCherry (Rb-mCherry; 5 x 10^8 TU/mL). **B.** Injection of the two Cre-dependent helper viruses at stock concentrations (AAV-TVA: 1 x 10^{13} GC/mL; AAV-RbG: 2 x 10^{13} GC/mL) followed by Rb-mCherry (5 x 10^7 TU/mL) in wild-type (WT) animals showed large Rb infection at the level of the injection site. No evidence of TVA:YFP or RbG-BFP fluorescence was observe, nor could we find evidence for transsynaptic spread to sites distal to injection in wild-type mice. Dilution of AAV-TVA by several orders of magnitude (2.4 x 10^{10} GC/mL) was required to minimize local infection in WT while allowing for robust transynpatic spread in Cre-expressing mouse lines as shown in Figure 1. scale= 500 μm **C.** Injection of AAV-TVA (2.4 x 10^{10} GC/mL) and Rb-mCherry (5 x 10^7 TU/mL) in Cre-expressing animals led to a modest infection at the injection site (VTA). Fibers, but no cell bodies were observed in afferent VTA-regions indicating retrograde transport of dilute AAV-TVA did not allow for direct Rb-mCherry infection. Inserts show LHb and LH regions at higher magnification; scale= 100 μm for afferent regions (LHb and LH).

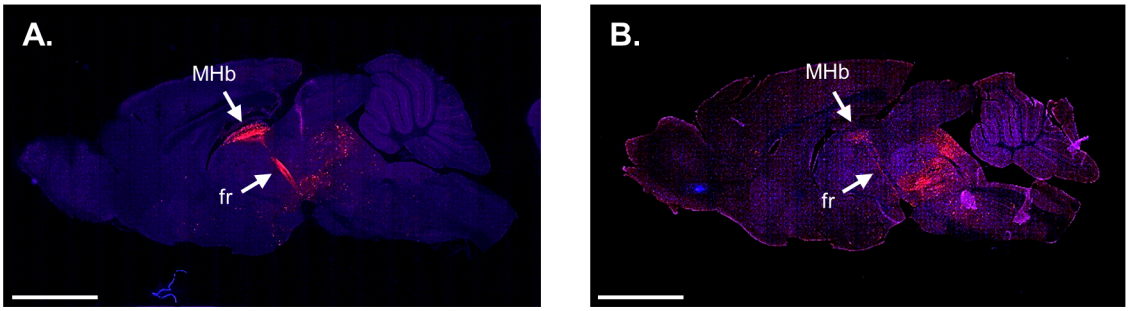

Figure S2, related to Figure 1. Comparison of VTA-restricted starter cells versus extra-VTA spread of starter cells in VGAT-Cre mice. **A**. Example image of sagittal section in a VGAT-Cre mouse that had substantial spread of starter cells localized in the interpeduncular nucleus ventral to medial VTA. Transsynaptic Rb-mCherry infection is clearly visible (red) in the medial habenula (MHb) and in the central portion of the fasciculus retroflexus (fr). **B**. An example sagittal section taken from a VGAT-Cre animal presenting starter cells well-restricted to the VTA. Only the exterior part of the fr is labeled show rabies positive fibers and rare rabies infected cells present in the MHb. Scale = 2.5mm.

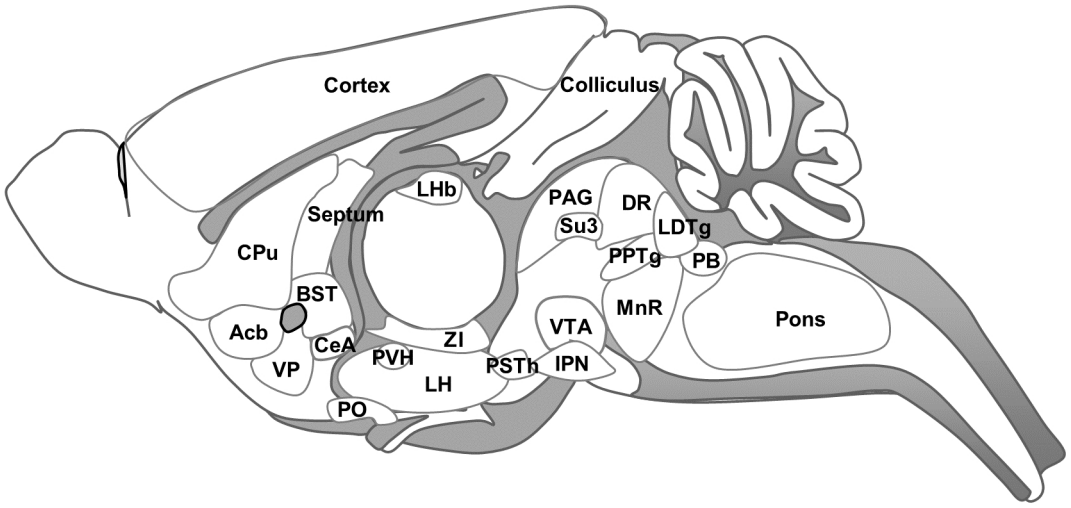

Figure S3, Brain region key to Figure 4D. Acb: nucleus accumbens, BST: bed nucleus of the stria terminalis, CeA: central amygdaloid nucleus, CPu: caudate putamen, DR: dorsal raphe nucleus, IPN: interpeduncular nucleus, LDTg: laterodorsal tegmental nucleus, LH: lateral hypothalamic area, LHb: lateral habenular nucleus, MnR: median raphe nucleus, PAG: periaqueductal gray, PB: parabrachial nucleus, PO: preoptic nucleus, PPTg: pedunculopontine tegmental nucleus, PSTH: parasubthalamic nucleus, PVH: Paraventricular hypothalamus, Su3: supraoculomotor periaqueductal gray, VP: ventral pallidum, VTA: ventral tegmental area, ZI: zona incerta. Figure S3 relates to Figure 4D.

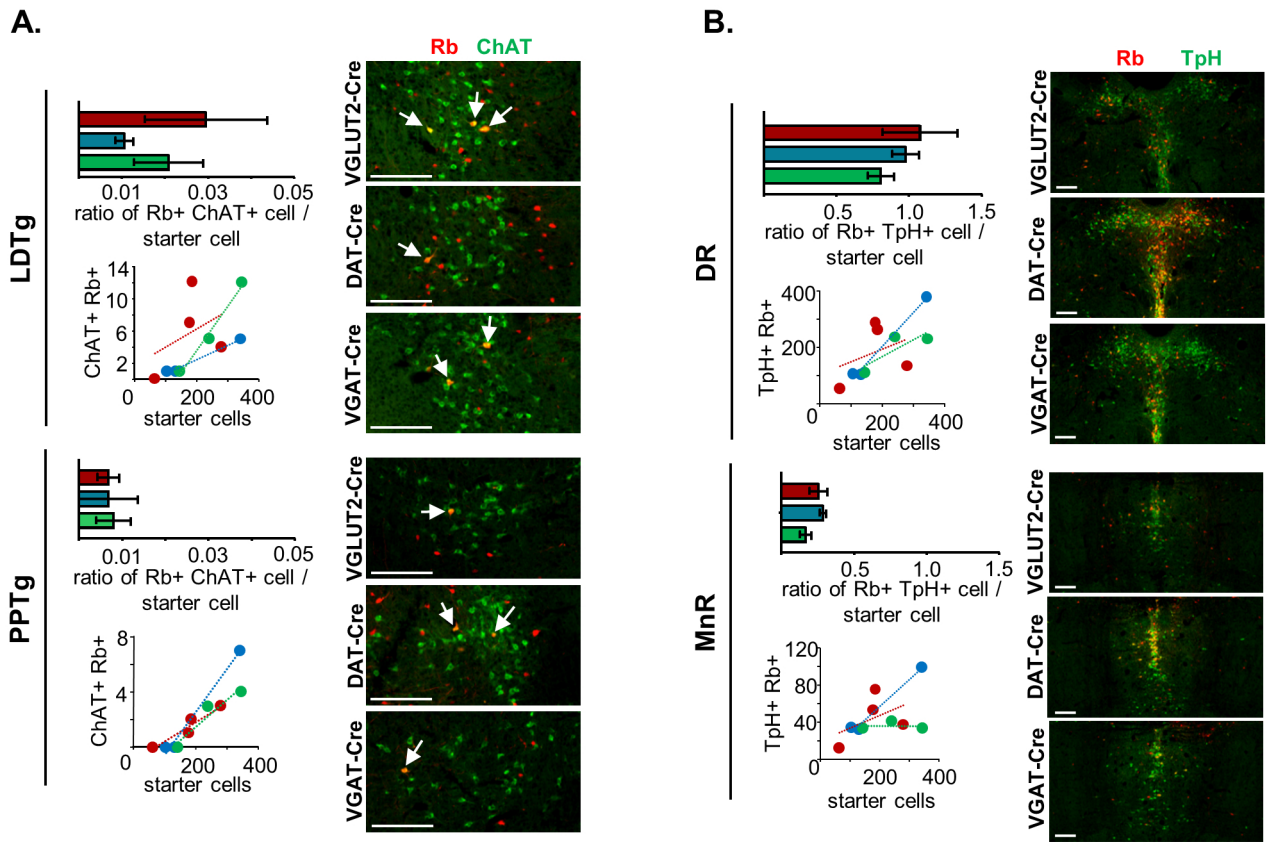

Figure S4, related to Figure 6. Immunohistochemical characterization of inputs to VTA from midbrain and hindbrain. **A**. Quantification of laterodorsal tegmental (LDTg; top) and pedunculopontine tegmental (PPTg; bottom) cholinergic afferents to transmitter-defined VTA cell types. Histograms represent the ratio of Rb-mCherry^{+} cells immunolabeled with anti-choline acetyltransferase (ChAT) relative to the number of starter cells (± SEM). ChaT^{+} input cells are denoted by white arrows. **B**. Quantification of midbrain serotoninergic afferents to transmitter-defined VTA cell types. Histograms represent the ratio of Rb-mCherry+ cells immunolabeled with anti-tryptophan hydroxylase (TpH) relative to the number of starter cells in dorsal raphe (DR) and median raphe (bottom) (± SEM). Points in scatterplots represent individual animals and lines are linear regressions. Example coronal images for each genotype show Rb-mCherry expression (red) and ChAt or TpH immunostaining (green); scale = 200 µm**.**

Table S1: Group contrasts by area, related to Figure 5

	VGLUT2-iCre vs DAT-iCre			VGLUT2-iCre vs VGAT-iCre			DAT-iCre vs VGAT-iCre		
	Fold Change	p-value	adj. p-value	Fold Change	p-value	adj. p-value	Fold Change	p-value	adj. p-value
Cortex	0.600	0.140	0.713	0.976	0.017*	0.214	0.376	0.372	0.902
Fibers	0.475	0.270	0.886	0.029	0.947	1.000	-0.446	0.287	0.886
Hindbrain	0.136	0.457	0.905	-0.557	0.002**	0.046*	-0.693	< .001***	0.016*
Hypothalamus	0.091	0.571	0.952	0.161	0.315	0.886	0.07	0.683	0.975
Midbrain	0.185	0.135	0.710	-0.042	0.731	0.976	-0.227	0.085	0.535
Pallidum	-0.371	0.102	0.612	0.174	0.446	0.904	0.545	0.024*	0.263
Striatum	-1.154	< .001***	0.020*	0.274	0.423	0.902	1.428	< .001***	0.006**
Thalamus	0.066	0.826	0.978	-1.064	< .001***	0.016*	-1.13	< .001***	0.016*

Table S2: Overall test for any group contrast (LRT) by area, related to Figure 5

	p-value	adj. p-value
Cortex	0.055	0.435
Fibers	0.409	0.902
Hindbrain	< .001***	0.017*
Hypothalamus	0.596	0.957
Midbrain	0.185	0.811
Pallidum	0.065	0.468
Striatum	< .001***	0.006**
Thalamus	< .001***	0.006**

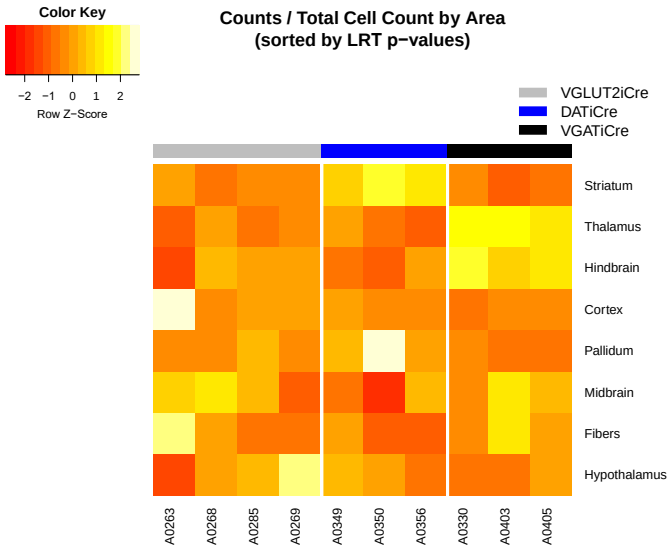

Table S3: Group contrasts by subarea, related to Figure 5

	VGLUT2-iCre vs DAT-iCre			VGLUT2-iCre vs VGAT-iCre			DAT-iCre vs VGAT-iCre		
	Fold Change	p-value	adj. p-value	Fold Change	p-value	adj. p-value	Fold Change	p-value	adj. p-value
Amygdalar nucleus	0.095	0.791	0.976	0.389	0.284	0.886	0.294	0.443	0.903
Claustrum	-0.043	0.938	1.000	-0.125	0.819	0.976	-0.082	0.882	0.995
Endopiriform nucleus	0.197	0.729	0.976	0.441	0.437	0.903	0.244	0.664	0.974
Hippocampal formation	0.848	0.106	0.623	0.914	0.081	0.529	0.065	0.897	1.000
Isocortex	1.008	0.058	0.439	1.157	0.030*	0.299	0.149	0.784	0.976
Olfactory	0.464	0.378	0.902	1.023	0.054	0.434	0.559	0.306	0.886
fibers	0.694	0.222	0.849	-0.055	0.923	1.000	-0.749	0.184	0.811
Medulla	0.141	0.739	0.976	-0.113	0.790	0.976	-0.254	0.567	0.949
Pons	0.154	0.425	0.902	-0.831	< .001***	0.002**	-0.984	< .001***	< .001***
Lateral zone	0.040	0.845	0.980	-0.003	0.990	1.000	-0.042	0.845	0.980
Medial zone	0.628	0.036*	0.327	0.088	0.767	0.976	-0.540	0.090	0.562
Periventricular zone	-0.104	0.759	0.976	-0.186	0.587	0.956	-0.081	0.822	0.976
Behavioral state related	0.242	0.289	0.886	-0.433	0.058	0.439	-0.675	0.005**	0.098
motor related	0.140	0.458	0.905	0.133	0.480	0.918	-0.007	0.974	1.000
Sensory related	0.127	0.714	0.976	0.402	0.249	0.860	0.275	0.455	0.905
Caudal region	-0.487	0.247	0.860	-0.336	0.425	0.902	0.151	0.732	0.976
Dorsal region	-0.933	0.071	0.484	0.232	0.656	0.974	1.165	0.029*	0.297
Medial region	0.228	0.684	0.975	-0.018	0.974	1.000	-0.247	0.664	0.974
Ventral region	-0.191	0.520	0.936	0.067	0.822	0.976	0.258	0.413	0.902
Lateral septal complex	0.533	0.330	0.886	0.346	0.527	0.936	-0.187	0.738	0.976
Striatum dorsal	-1.499	0.007**	0.121	0.712	0.203	0.828	2.212	< .001***	0.006**
Striatum ventral	-1.049	0.003**	0.055	-0.065	0.854	0.981	0.985	0.007**	0.123
Polymodal association	-0.017	0.955	1.000	-1.592	< .001***	< .001***	-1.575	< .001***	< .001***
Sensory-motor	0.302	0.549	0.941	0.245	0.627	0.974	-0.057	0.913	1.000

Table S4: Overall test for any group contrast (LRT) by subarea, related to Figure 5

	p-value	adj. p-value
Amygdalar nucleus	0.556	0.941
Claustrum	0.973	1.000
Endopiriform nucleus	0.722	0.976
Hippocampal formation	0.144	0.723
Isocortex	0.057	0.439
Olfactory	0.164	0.771
fibers	0.332	0.886
Medulla	0.849	0.980
Pons	< .001***	< .001***
Lateral zone	0.974	1.000
Medial zone	0.101	0.612
Periventricular zone	0.859	0.983
Behavioral state related	0.017*	0.215
motor related	0.690	0.976
Sensory related	0.511	0.936
Caudal region	0.489	0.930
Dorsal region	0.059	0.439
Medial region	0.885	0.995
Ventral region	0.690	0.976
Lateral septal complex	0.611	0.964
Striatum dorsal	< .001***	0.016*
Striatum ventral	0.003**	0.060
Polymodal association	< .001***	< .001***
Sensory-motor	0.806	0.976

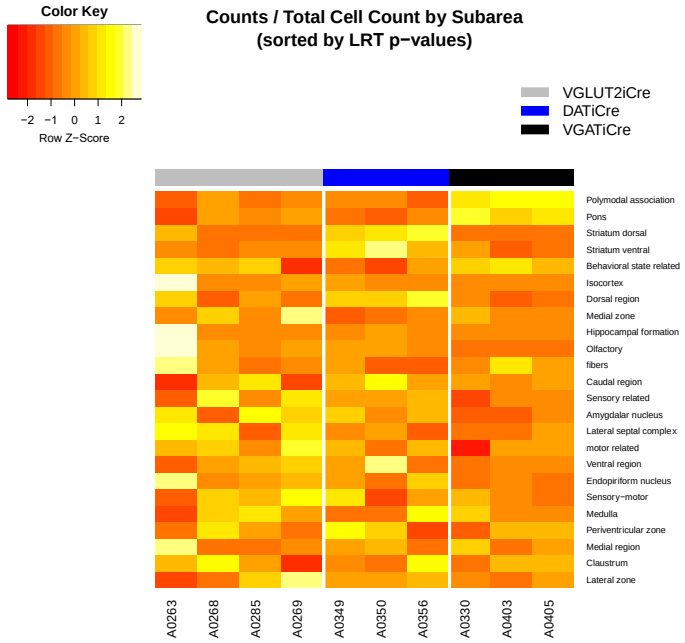

Table S5: Group contrasts by region (sorted by LRT p-values), related to Figure 5

	VGLUT2-iCre vs DAT-iCre			VGLUT2-iCre vs VGAT-iCre			DAT-iCre vs VGAT-iCre		
	Fold Change	p-value	adj. p-value	Fold Change	p-value	adj. p-value	Fold Change	p-value	adj. p-value
LDTg	0.156	0.699	0.976	-1.360	< .001***	0.017*	-1.517	< .001***	0.016*
sm	-0.504	0.581	0.954	-3.143	< .001***	0.016*	-2.639	0.004**	0.081
LHb	0.106	0.835	0.980	-1.620	0.001**	0.031*	-1.726	0.001**	0.031*
CPu	-1.956	0.021*	0.247	1.614	0.065	0.468	3.571	< .001***	0.006**
PVH	-0.535	0.211	0.839	1.188	0.012*	0.176	1.723	< .001***	0.017*
AcbSh	-0.850	0.029*	0.297	0.579	0.150	0.729	1.430	< .001***	0.020*
Tu	-0.188	0.819	0.976	3.112	< .001***	0.025*	3.300	< .001***	0.020*
AcbC	-2.043	0.001**	0.032*	-0.512	0.428	0.902	1.531	0.023*	0.255
InC	0.774	0.477	0.918	3.839	< .001***	0.022*	3.065	0.009**	0.144
PIL	0.000	1.000	1.000	-3.304	0.008**	0.126	-3.004	0.015*	0.198
DTg	-0.048	0.965	1.000	-2.800	0.010**	0.149	-2.752	0.014*	0.191
CM	-3.087	0.013*	0.183	0.000	1.000	1.000	2.743	0.025*	0.265
PDTg	-1.589	0.188	0.811	-3.276	0.006**	0.103	-1.686	0.156	0.743
Septum	2.916	0.006**	0.103	1.591	0.123	0.678	-1.326	0.231	0.851
LGP	-1.361	0.051	0.423	0.402	0.573	0.952	1.763	0.018*	0.221
S1/S2	2.140	0.035*	0.327	2.385	0.019*	0.227	0.245	0.819	0.976
RC	2.630	0.033*	0.321	2.623	0.033*	0.321	0.000	1.000	1.000
CA1/CA3	2.342	0.059	0.439	2.932	0.018*	0.221	0.590	0.634	0.974
PPTg	0.781	0.063	0.464	-0.354	0.390	0.902	-1.135	0.011*	0.160
SO	1.313	0.176	0.806	2.533	0.013*	0.186	1.220	0.258	0.875
RMg	0.540	0.528	0.936	-1.460	0.084	0.535	-2.000	0.025*	0.265
PrL	0.115	0.916	1.000	2.481	0.036*	0.327	2.366	0.049*	0.418
CeA	-1.191	0.021*	0.247	-0.554	0.292	0.886	0.637	0.244	0.858
Pir	0.833	0.436	0.903	2.678	0.016*	0.208	1.845	0.108	0.625
DLL	0.117	0.923	1.000	-2.265	0.068	0.478	-2.383	0.051	0.423
ATg	0.698	0.552	0.941	-1.837	0.114	0.644	-2.535	0.034*	0.321
VTg	1.526	0.127	0.697	-0.828	0.389	0.902	-2.354	0.023*	0.255
AAD	1.694	0.037*	0.327	1.100	0.169	0.784	-0.594	0.491	0.930
LAcbSh	-1.587	0.052	0.423	-0.345	0.676	0.975	1.242	0.147	0.729
Acb	-0.163	0.813	0.976	-1.214	0.067	0.477	-1.052	0.138	0.713
MD	-1.585	0.152	0.729	0.449	0.701	0.976	2.034	0.083	0.535
MA3	-0.991	0.417	0.902	-2.166	0.078	0.517	-1.175	0.335	0.886
M1	1.583	0.134	0.710	1.703	0.108	0.625	0.120	0.914	1.000
PL	0.639	0.328	0.886	-0.616	0.327	0.886	-1.255	0.066	0.474
LC	-0.393	0.404	0.902	-0.834	0.071	0.484	-0.441	0.369	0.899
Co	0.271	0.821	0.976	1.905	0.120	0.671	1.634	0.187	0.811
PAG	0.265	0.602	0.958	0.926	0.071	0.484	0.661	0.226	0.851
Cg	1.914	0.075	0.498	1.051	0.317	0.886	-0.862	0.442	0.903
Su3	-0.711	0.141	0.713	0.052	0.915	1.000	0.763	0.138	0.713
BLA	0.741	0.547	0.941	1.902	0.123	0.678	1.161	0.348	0.887
SubI	1.915	0.091	0.565	0.394	0.723	0.976	-1.521	0.192	0.815
GI/DI	1.864	0.103	0.613	1.001	0.375	0.902	-0.863	0.465	0.913
DTT	1.632	0.112	0.638	0.900	0.368	0.899	-0.732	0.499	0.932
Rh	-1.479	0.185	0.811	0.000	1.000	1.000	1.346	0.205	0.828
REth	1.911	0.113	0.640	0.997	0.401	0.902	-0.914	0.459	0.905
Po	0.394	0.751	0.976	1.646	0.183	0.811	1.252	0.309	0.886
all fiber tracts	1.493	0.131	0.710	0.018	0.985	1.000	-1.475	0.152	0.729
APT	1.361	0.199	0.828	1.382	0.194	0.820	0.021	0.985	1.000
I3	0.000	1.000	1.000	-1.426	0.200	0.828	-1.303	0.218	0.849
Pr5	0.222	0.849	0.980	1.762	0.140	0.713	1.541	0.206	0.828
CnF	1.239	0.169	0.784	-0.172	0.844	0.980	-1.411	0.133	0.710
CGA	-0.696	0.334	0.886	-1.062	0.136	0.710	-0.366	0.622	0.971
Eth	1.308	0.239	0.858	1.305	0.240	0.858	0.000	1.000	1.000
MnR	-0.018	0.967	1.000	-0.566	0.186	0.811	-0.548	0.230	0.851
SuM	0.645	0.246	0.860	-0.204	0.709	0.976	-0.849	0.149	0.729
VLTg	-0.349	0.777	0.976	1.071	0.381	0.902	1.420	0.241	0.858
DMH/VMH	0.007	0.988	1.000	-0.604	0.203	0.828	-0.611	0.229	0.851
PC	-1.260	0.297	0.886	-1.351	0.264	0.879	-0.091	0.939	1.000
CGPn	0.897	0.302	0.886	-0.422	0.613	0.964	-1.318	0.145	0.723

Table S5 (continued): Group contrasts by region (sorted by LRT p-values), related to Figure 5

	VGLUT2-iCre vs DAT-iCre			VGLUT2-iCre vs VGAT-iCre			DAT-iCre vs VGAT-iCre		
	Fold Change	p-value	adj. p-value	Fold Change	p-value	adj. p-value	Fold Change	p-value	adj. p-value
PH	0.651	0.150	0.729	0.303	0.499	0.932	-0.349	0.471	0.918
AC	-0.491	0.692	0.976	0.972	0.427	0.902	1.463	0.228	0.851
DLO	-1.255	0.251	0.863	0.000	1.000	1.000	1.140	0.267	0.886
AH/LA	0.136	0.862	0.983	1.073	0.182	0.811	0.937	0.269	0.886
RS	1.165	0.308	0.886	1.460	0.205	0.828	0.295	0.805	0.976
DB	-1.034	0.237	0.858	-1.064	0.223	0.849	-0.030	0.974	1.000
TC	-1.330	0.221	0.849	-0.215	0.845	0.980	1.114	0.321	0.886
MiTg	1.511	0.171	0.789	0.312	0.773	0.976	-1.198	0.293	0.886
DTM	1.156	0.289	0.886	1.154	0.288	0.886	0.000	1.000	1.000
IL	-1.597	0.184	0.811	-0.951	0.432	0.903	0.646	0.595	0.957
Ventral N Thalamus	-0.086	0.921	1.000	1.077	0.235	0.858	1.164	0.219	0.849
PCOm	1.444	0.243	0.858	1.307	0.290	0.886	-0.138	0.912	1.000
DK	1.241	0.201	0.828	0.164	0.860	0.983	-1.077	0.288	0.886
Arc	-0.734	0.257	0.875	-0.754	0.244	0.858	-0.020	0.976	1.000
EMi	1.291	0.273	0.886	0.790	0.506	0.936	-0.500	0.661	0.974
PR	1.046	0.249	0.860	0.844	0.349	0.887	-0.202	0.835	0.980
DpMe	0.674	0.278	0.886	0.654	0.291	0.886	-0.019	0.977	1.000
BST	-0.603	0.213	0.841	-0.316	0.514	0.936	0.286	0.576	0.952
LOT	-0.032	0.979	1.000	1.122	0.357	0.887	1.154	0.338	0.886
M2	0.818	0.368	0.899	1.046	0.254	0.868	0.228	0.815	0.976
IRt	1.380	0.224	0.849	0.886	0.430	0.902	-0.494	0.677	0.975
LPtA	0.000	1.000	1.000	-1.111	0.301	0.886	-0.988	0.336	0.886
AI	0.667	0.419	0.902	0.982	0.243	0.858	0.315	0.726	0.976
VO	-0.671	0.523	0.936	0.703	0.525	0.936	1.374	0.224	0.849
MM	0.626	0.327	0.886	0.666	0.298	0.886	0.039	0.954	1.000
Ect	1.302	0.284	0.886	1.150	0.343	0.887	-0.152	0.902	1.000
Xi	-1.044	0.327	0.886	0.000	1.000	1.000	0.929	0.354	0.887
Gi	0.883	0.262	0.877	0.652	0.404	0.902	-0.231	0.784	0.976
PBG	1.038	0.338	0.886	1.043	0.330	0.886	0.000	1.000	1.000
Ve	0.688	0.507	0.936	1.189	0.260	0.875	0.501	0.651	0.974
VLGMC	-0.634	0.589	0.956	0.497	0.667	0.974	1.131	0.317	0.886
PT	-0.992	0.350	0.887	0.000	1.000	1.000	0.875	0.380	0.902
Sub	0.587	0.607	0.963	1.039	0.359	0.890	0.451	0.680	0.975
PC5	0.166	0.879	0.995	-0.902	0.419	0.902	-1.068	0.314	0.886
colliculus	-0.005	0.991	1.000	0.461	0.312	0.886	0.466	0.337	0.886
Lateral Septum	0.700	0.307	0.886	0.540	0.429	0.902	-0.160	0.830	0.979
P5	-1.215	0.325	0.886	-0.117	0.924	1.000	1.098	0.368	0.899
LaA	0.794	0.481	0.918	1.050	0.346	0.887	0.256	0.809	0.976
DMTg	0.828	0.435	0.903	1.086	0.308	0.886	0.257	0.817	0.976
PP	0.449	0.687	0.976	-0.501	0.659	0.974	-0.951	0.382	0.902
SubC	0.238	0.834	0.980	1.198	0.301	0.886	0.959	0.420	0.902
DEn/VEn	0.269	0.756	0.976	0.873	0.336	0.886	0.603	0.530	0.936
Su5	-0.258	0.823	0.976	-1.170	0.318	0.886	-0.911	0.424	0.902
RPO	-0.208	0.863	0.983	0.756	0.520	0.936	0.964	0.402	0.902
CxA	0.545	0.610	0.964	1.056	0.329	0.886	0.511	0.650	0.974
FrA	0.369	0.748	0.976	0.911	0.422	0.902	0.542	0.620	0.970
SubB	-0.062	0.959	1.000	-1.021	0.390	0.902	-0.959	0.429	0.902
BAC	0.806	0.452	0.905	0.813	0.439	0.903	0.000	1.000	1.000
BMA	0.518	0.674	0.974	1.178	0.340	0.887	0.659	0.596	0.957
Re	-0.510	0.648	0.974	0.375	0.732	0.976	0.886	0.405	0.902
PB	0.148	0.708	0.976	-0.241	0.540	0.940	-0.390	0.354	0.887
VP/SI	-0.231	0.534	0.936	0.136	0.715	0.976	0.366	0.355	0.887
MCPC	0.081	0.943	1.000	0.712	0.522	0.936	0.631	0.556	0.941
MGP	0.350	0.722	0.976	0.879	0.381	0.902	0.530	0.615	0.966
Rt	0.672	0.588	0.956	1.120	0.367	0.899	0.448	0.718	0.976
PM	-0.486	0.533	0.936	0.238	0.765	0.976	0.724	0.384	0.902
RtTg	-0.463	0.562	0.944	-0.693	0.383	0.902	-0.230	0.782	0.976
STh/PSTh	-0.361	0.563	0.945	-0.547	0.380	0.902	-0.186	0.778	0.976
Ew/3PC/3N	-0.610	0.552	0.941	-0.877	0.390	0.902	-0.268	0.800	0.976

Table S5 (continued): Group contrasts by region (sorted by LRT p-values), related to Figure 5

	VGLUT2-iCre vs DAT-iCre			VGLUT2-iCre vs VGAT-iCre			DAT-iCre vs VGAT-iCre		
	Fold Change	p-value	adj. p-value	Fold Change	p-value	adj. p-value	Fold Change	p-value	adj. p-value
Pa4	0.143	0.752	0.976	-0.251	0.576	0.952	-0.395	0.413	0.902
RI	-0.795	0.522	0.936	0.177	0.887	0.995	0.971	0.434	0.903
PF	0.500	0.480	0.918	0.438	0.534	0.936	-0.062	0.935	1.000
MO	-0.492	0.673	0.974	0.465	0.696	0.976	0.957	0.428	0.902
LEnt	-0.409	0.709	0.976	0.337	0.752	0.976	0.746	0.467	0.914
Gus	-0.262	0.812	0.976	0.442	0.681	0.975	0.705	0.497	0.932
SFO	0.301	0.779	0.976	-0.391	0.718	0.976	-0.692	0.501	0.933
PCRt	0.448	0.673	0.974	0.827	0.445	0.904	0.379	0.738	0.976
LO	0.748	0.476	0.918	0.563	0.590	0.956	-0.185	0.867	0.986
LPO/MPO/MPA	0.031	0.956	1.000	-0.362	0.523	0.936	-0.393	0.514	0.936
I	-0.014	0.990	1.000	0.516	0.628	0.974	0.530	0.601	0.958
ZI	0.314	0.557	0.941	0.321	0.549	0.941	0.006	0.991	1.000
MCPO	-0.140	0.802	0.976	0.261	0.645	0.974	0.401	0.504	0.936
F	0.858	0.489	0.930	0.349	0.779	0.976	-0.510	0.680	0.975
V2	0.309	0.774	0.976	0.637	0.547	0.941	0.328	0.743	0.976
DR	0.181	0.662	0.974	-0.119	0.773	0.976	-0.300	0.495	0.932
IPAC	-0.480	0.538	0.940	-0.086	0.912	1.000	0.394	0.631	0.974
SPTg	-0.305	0.674	0.974	-0.451	0.533	0.936	-0.147	0.847	0.980
MeA	0.369	0.756	0.976	0.739	0.535	0.936	0.370	0.761	0.976
A8/RRF	-0.376	0.597	0.957	-0.394	0.579	0.952	-0.018	0.981	1.000
IG	0.447	0.669	0.974	0.442	0.667	0.974	0.000	1.000	1.000
Pr	0.447	0.669	0.974	0.442	0.667	0.974	0.000	1.000	1.000
Sp5	0.447	0.669	0.974	0.442	0.667	0.974	0.000	1.000	1.000
KF	0.369	0.765	0.976	-0.355	0.773	0.976	-0.724	0.560	0.943
Sfi	0.650	0.599	0.958	0.171	0.889	0.997	-0.478	0.701	0.976
AOM	-0.039	0.971	1.000	0.352	0.735	0.976	0.391	0.693	0.976
RR	0.200	0.870	0.988	-0.449	0.713	0.976	-0.649	0.590	0.956
LH/MCLH	0.001	0.996	1.000	0.134	0.642	0.974	0.132	0.667	0.974
ADP	0.458	0.712	0.976	-0.064	0.959	1.000	-0.523	0.673	0.974
DP	-0.146	0.852	0.980	0.163	0.837	0.980	0.309	0.713	0.976
PV	-0.020	0.983	1.000	0.347	0.704	0.976	0.367	0.702	0.976
Icj	-0.402	0.722	0.976	-0.352	0.755	0.976	0.050	0.963	1.000
MG	0.069	0.955	1.000	0.391	0.749	0.976	0.321	0.789	0.976
Mtu	-0.307	0.789	0.976	0.076	0.947	1.000	0.383	0.744	0.976
Anterior N Thalamus	0.289	0.811	0.976	0.229	0.850	0.980	-0.061	0.959	1.000
Pn	0.055	0.911	1.000	-0.105	0.829	0.979	-0.160	0.758	0.976
S	-0.012	0.991	1.000	-0.247	0.820	0.976	-0.235	0.820	0.976
ILL	0.145	0.898	1.000	0.165	0.884	0.995	0.020	0.986	1.000
Cl	-0.097	0.887	0.995	-0.132	0.846	0.980	-0.035	0.962	1.000
PrC	0.163	0.894	1.000	0.147	0.905	1.000	-0.016	0.989	1.000

Table S6: Overall test for any group contrast (LRT) by region, related to Figure 5

	p-value	adj. p-value
LDTg	< .001***	0.008**
sm	< .001***	0.017*
LHb	< .001***	0.017*
CPu	< .001***	0.020*
PVH	0.002**	0.050*
AcbSh	0.002**	0.053
Tu	0.003**	0.056
AcbC	0.003**	0.059
InC	0.004**	0.081
PIL	0.010**	0.151
DTg	0.012*	0.168
CM	0.019*	0.227
PDTg	0.024*	0.265
Septum	0.030*	0.302
LGP	0.034*	0.321
S1/S2	0.035*	0.327
RC	0.037*	0.327
CA1/CA3	0.038*	0.33
PPTg	0.040*	0.341
SO	0.045*	0.382
RMg	0.053	0.432
PrL	0.058	0.439
CeA	0.069	0.481
Pir	0.074	0.498
DLL	0.082	0.529
ATg	0.087	0.545
VTg	0.095	0.584
AAD	0.102	0.612
LAcbSh	0.112	0.638
Acb	0.132	0.71
MD	0.154	0.738
MA3	0.159	0.75
M1	0.184	0.811
PL	0.19	0.814
LC	0.191	0.815
Co	0.2	0.828
PAG	0.208	0.833
Cg	0.214	0.844
Su3	0.219	0.849
BLA	0.244	0.858
SubI	0.26	0.875
GI/DI	0.274	0.886
DTT	0.28	0.886
Rh	0.282	0.886
REth	0.284	0.886
Po	0.289	0.886
all fiber tracts	0.293	0.886
APT	0.295	0.886
I3	0.302	0.886
Pr5	0.309	0.886
CnF	0.31	0.886
CGA	0.313	0.886
Eth	0.322	0.886
MnR	0.335	0.886
SuM	0.341	0.887
VLTg	0.345	0.887
DMH/VMH	0.349	0.887
PC	0.353	0.887
CGPn	0.357	0.887

	p-value	adj. p-value
PH	0.357	0.887
AC	0.377	0.902
DLO	0.388	0.902
AH/LA	0.392	0.902
RS	0.392	0.902
DB	0.396	0.902
TC	0.399	0.902
MiTg	0.401	0.902
DTM	0.413	0.902
IL	0.416	0.902
Ventral N Thalamus	0.418	0.902
PCOm	0.418	0.902
DK	0.422	0.902
Arc	0.424	0.902
EMi	0.442	0.903
PR	0.443	0.903
DpMe	0.443	0.903
BST	0.453	0.905
LOT	0.453	0.905
M2	0.455	0.905
IRt	0.455	0.905
LPtA	0.455	0.905
AI	0.459	0.905
VO	0.469	0.916
MM	0.476	0.918
Ect	0.477	0.918
Xi	0.480	0.918
Gi	0.496	0.932
PBG	0.496	0.932
Ve	0.514	0.936
VLGMC	0.516	0.936
PT	0.519	0.936
Sub	0.526	0.936
PC5	0.527	0.936
colliculus	0.542	0.941
Lateral Septum	0.543	0.941
P5	0.552	0.941
LaA	0.553	0.941
DMTg	0.554	0.941
PP	0.576	0.952
SubC	0.577	0.952
DEn/VEn	0.579	0.952
Su5	0.584	0.956
RPO	0.592	0.957
CxA	0.601	0.958
FrA	0.610	0.964
SubB	0.620	0.970
BAC	0.627	0.974
BMA	0.633	0.974
Re	0.639	0.974
PB	0.641	0.974
VP/SI	0.642	0.974
MCPC	0.646	0.974
MGP	0.647	0.974
Rt	0.651	0.974
PM	0.665	0.974
RtTg	0.668	0.974
STh/PSTh	0.669	0.974
Ew/3PC/3N	0.691	0.976

Table S6 (continued): Overall test for any group contrast (LRT) by region, related to Figure 5

	p-value	adj. p-value
Pa4	0.699	0.976
RI	0.700	0.976
PF	0.717	0.976
MO	0.726	0.976
LEnt	0.727	0.976
Gus	0.733	0.976
SFO	0.736	0.976
PCRt	0.743	0.976
LO	0.752	0.976
LPO/MPO/MPA	0.753	0.976
I	0.776	0.976
ZI	0.778	0.976
MCPO	0.781	0.976
F	0.783	0.976
V2	0.784	0.976
DR	0.791	0.976
IPAC	0.807	0.976
SPTg	0.812	0.976
MeA	0.814	0.976
A8/RRF	0.817	0.976
IG	0.820	0.976
Pr	0.820	0.976
Sp5	0.820	0.976
KF	0.843	0.980
Sfi	0.846	0.980
AOM	0.853	0.980
RR	0.858	0.983
LH/MCLH	0.878	0.995
ADP	0.884	0.995
DP	0.902	1.000
PV	0.907	1.000
Icj	0.923	1.000
MG	0.933	1.000
Mtu	0.940	1.000
Anterior N Thalamus	0.949	1.000
Pn	0.951	1.000
S	0.956	1.000
ILL	0.967	1.000
Cl	0.972	1.000
PrC	0.980	1.000

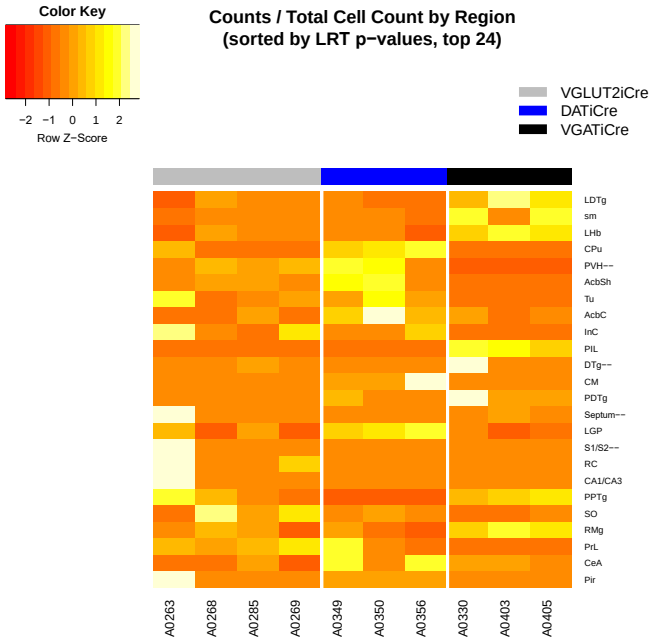

File S1, related to Figure 2, 3 and 4

Supplemental Experimental procedures

Animals. Homozygous breeders for VGLUT2-IRES-Cre (Vong et al., 2011), VGAT-IRES-Cre (Vong et al., 2011) and DAT-IRES-Cre (Backman et al., 2006) were obtained from The Jackson Laboratory: *Slc17a6*$^{tm2(cre)Lowl}$ (stock no: 016963), *Slc32a1*$^{tm2(cre)Lowl}$ (stock no: 016962), and *Slc6a3*$^{tm1.1(cre)Bkmn}$ (stock no: 006660). Control mice were wild-type littermates obtained by back-crossing with C57Bl/6 mice (The Jackson Laboratory). Note that VGLUT2-Cre and DAT-Cre were fully backcrossed to C57Bl/6 but VGAT-Cre mice are on a mixed 129Sv x C57Bl/6. Mice were bred at UCSD, group housed, and maintained on a 12h light-dark cycle with food and water available *ad libitum*. Both male and female mice were included and all experiments performed in accordance with protocols approved by the University of California San Diego Institutional Animal Care and Use Committee.

Viruses and stereotaxic surgery. Plasmid construction and virus production of Rb-ΔG-mCherry were described in our previous studies (Osakada and Callaway, 2013; Osakada et al., 2011). For construction of pAAV-CMV-Syn-DIO-TVA950-EYFP, CMV enhancer and synapsin I promoter were cloned by PCR (Hioki et al., 2007).TVA950 was fused with EYFP with In-Fusion reaction. For construction of AAV1-EF1α-DIO-H2B-tagBFP-Flagx3-T2Am-cB19G, N-terminus and C-terminus of tagBFP were fused with Histone 2B and three tandem FLAG epitopes, respectively. ORF of rabies glycoprotein was codon-optimized for mice and humans and synthesized to obtain cB19G. The N terminus and C-terminus of T2A were modified by addition of GSG and APGS, respectively (Tang et al., 2009). Rb and AAV vectors were obtained from the Salk Gene Transfer Targeting and Therapeutics Core. For intracranial injection, mice (5-6 weeks old) were deeply anesthetized with isoflurane, placed in a 1900-model Kopf Stereotaxic apparatus (Kopf Instruments, Tujunga, California) and 200 nL of 1:1 mixture AAV2/1-CMVeSyn-DIO-TVA950-EYFP (AAV-TVA; 2.4 x 10^{10} GC/mL unless noted) and AAV2/1-EF1α -DIO-H2B-tagBFP-Flagx3-T2Am-cB19G (AAV-RbG; 1.1 x 10^{13} GC/mL) prepared in HBSS 1X (Hanks' balanced salt solution, Gibco), infused unilaterally into the left hemisphere VTA (LM= -0.4, AP= -3.4, DV= -4.4; mm relative to Bregma) at 100 nl/min (WPI UltraMicroPump) using custom-made 30-gauge stainless (Plastics One, VA) injectors. The injection tip was left in place for an additional 10 min then slowly retracted. Animals were allowed to recover for 3 to 4 weeks to enable optimal virus expression. Then 125 nL of EnvA-Rb-ΔG-mcherry (Rb-mCherry; 5 x 10^{7} TU/mL) were injected at the same stereotaxic coordinates following the same procedure. Control experiments included injections of these 3 viruses in wild-type littermates, injection of only Rb-mCherry in Cre-expressing animals, and injection of only AAV-TVA and Rb-mcherry in each of the Cre-expressing mouse lines.

Histology. Seven days after injection of Rb-mCherry, mice were deeply anesthetized with a mixture of ketamine (Pfizer, 10 mg/kg i.p.) and xylazine (LLOYD, 2 mg/kg i.p.) and transcardially perfused with 10 ml of phosphate buffered saline (PBS) followed by 50 ml 4% paraformaldehyde (PFA) at a rate of 5-6 ml/min. Brains were extracted, incubated in 4% PFA at 4ºC overnight then transferred to 30% sucrose solution in PBS for 48 to 70 hours at 4ºC. Brains were snap frozen in isopentane and stored at -80ºC. For quantitative assessments, 30-µm coronal cryo-sections were cut using a cryostat (CM3050S, Leica) and collected in a solution of 0.01% sodium azide PBS. An additional cohort of animals was used to collect 50-µm sagittal cryo-sections for visualization but were not counted.

For immunostaining, brain sections were gently rocked and washed 3x 5 min in PBS, 3x 5 min in PBS containing 0.2 % triton X-100 (PBS-Tx), and blocked with 4% normal donkey serum (NDS) in PBS-Tx (blocking) for 1 hour at room temperature (RT). Sections were then incubated in blocking solution at 4ºC overnight using one or more of the following primary antibodies: rabbit anti-TH, 1:2000, Millipore AB152; sheep anti-TH, 1:2000, Pel-Freez P60101-0; mouse anti-Flag M2, 1:2000, Sigma F3165; goat anti-ChAT, 1:400, Millipore AB144P; sheep anti-αTpH (αTryptophan hydroxylase), 1:2000, Pel Freeze P60401-0; rat anti-substance P, 1:400, Millipore MAB356, mouse anti-parvalbumin, 1:2000, Millipore MAB1572; goat anti-Orexin-A (C-19), 1:1000, Santa Cruz Biotechnology sc-8070, goat anti-pro-MCH (C-20), 1:1000, Santa Cruz Biotechnology sc-14509; mouse anti-Oxytocin, 1:500, Millipore MAB5296. Sections were rinsed 3x 10min with PBS-Tx and incubated in appropriate secondary antibodies (Jackson ImmunoResearch) conjugated to Alexa488 or Alexa647 fluorescent dyes (5 □g/ml) for 2 hr at RT. Sections were washed 3x 10 min with PBS, mounted on to slides and coverslipped with Fluoromount-G mounting medium (Southern Biotech) ± DAPI (Roche, 0.5 □g/ml).

Imaging. Images for counting starter cells were acquired with a 4x magnification (NA: 0.16) objective using an Olympus BX53 epifluorescence microscope (equipped with a Hamamatsu ORCA-Flash4 camera) and CellSens dimension 1.12 software and at 10x magnification (NA: 0.45) objective using a Zeiss AxioObserver Z1 widefield epifluorescence microscope and Zen blue Zeiss software (2012 version). Afferent input counting and most of the immunohistochemical characterization of afferent inputs was realized on images acquired with the slide scanner NanoZoomer 2 HT and fluorescence module L10387-03 (Hamamatsu Photonics, Japan). Acquisition was performed using a dry 20x objective (NA: 0.75). 40x resolution was achieved with a lens converter. Images for immunohistochemical characterization were also acquired using the Zeiss AxioObserver Z1 widefield epifluorescence microscope at 10x (NA: 0.45) and 20x (NA: 0.75) magnifications. ApoTome 2.0 technology was used with 20x objective for structured illumination.

Cell counts. Counting of starter cells, afferent input cells and immunohistochemically-characterized cells was conducted manually on one 30-µm section every 150µm along the rostral caudal extent of the brain. Starter cells in the VTA were counted manually and blindly using the cell counter plugin of ImageJ software from Bregma -2.8mm to -4.36mm. Cells were considered as starter cells when expressing native cytoplasmic mCherry fluorescence (EnvA-Rb-ΔG-mCherry) and nuclear immunolabel against the Flag epitope on RbG (AAV2/1-EF1α-DIO-hBFP-Flagx3-T2Am-B19G). Five to six animals per group were injected with the helper AAV and Rb vectors. Coronal sections for starter cell counts were co-labeled with TH to assist in drawing VTA boundaries. Whole-brain labor-intensive cell counts were not completed on mice presenting large numbers of starter cells outside of the VTA. The remaining 3-4 animals used per group presented none or less than 3% starter cells outside the VTA for GABA and glutamate-expressing starter cells, and less than 10% for dopamine-expressing starter cells. For the DAT-IRES-Cre, VGLUT2-IRES-Cre and VGAT-IRES-Cre animals respectively rare or few starters were observed; in the substantia nigra pars compacta (SNC) and the retrorubral field (A8); in the supramammillary nucleus (SuM) and posterior hypothalamus (PH); and in the interpeduncular nucleus (IP) (**File S1**). Tyrosine Hydroxylase (TH)-positive starter cells were counted on the same sections and identified as TH positive when soma and cell processes fully overlapped for TH immunolabel and native mCherry.

Afferent inputs were manually and blindly counted on screen using the NDP viewer with an integrated high-resolution zoom and equipped with a counting tool. Counting was realized from Bregma +2.8mm to -5.8mm on 53 +/- 0.5 sections. Neurons were considered as VTA afferent inputs when the red fluorescence (mCherry) was filling objects that showed clear borders and processes. Regions were identified by a single investigator and using the Paxinos Mouse Brain Atlas (Paxinos & Franklin 2001) as reference. Regions were grouped into areas and sub-areas based on the Allen Brain Atlas classification (http://mouse.brain-map.org/).

Immunochemical characterization of inputs was performed manually and blindly using the NDP viewer and/or the cell counter plugin of ImageJ. Cells were considered immunopositive for a specific marker when the AlexaFluor488 (fluorophore of the secondary antibody immunolabel) was clearly overlapping mCherry. ChAT immunofluorescence was counted in the PPTg from Bregma -4.2 mm to -5.0 mm; and in the LDTg from Bregma -4.8 mm to -5.5 mm. TpH immunoreactivity was measured in the DR from Bregma -4.0 mm to -5.3 mm; and in the MnR from Bregma -4.0 mm to -5.0 mm. In the LH, we used separate sections to assess Orexin or MCH expression from Bregma -0.3 mm to -2.8 mm. Parvalbumin staining in the VP was counted from Bregma +1.9 mm to -0.3 mm.

Statistics. All data were assessed using one-way ANOVA with cell type as a factor and Tukey's posthoc test to correct for multiple comparisons. Because different regions had widely variable inputs to VTA, we used two complimentary approaches to analyze differences in the proportions of input each area/region sends to each VTA cell type. As represented in **Figure 4**, we ran one-way ANOVAs with Tukey's posthoc test to correct for multiple cell-type comparisons on each of the seven areas assessed and select sub-areas or regions (representing the top 25 inputs). No corrections were made to account for running these 32 ANOVAs. As represented in **Figure 5** we adopted a transcriptomic analysis strategy to model the difference in cell counts between each group within each area, subarea, or region. In light of possible overdispersion, we fitted negative binomial models using the methods of Love, Huber, and Anders (Love et al., 2014) and the package DESeq, and report each pairwise comparison (i.e. DAT-Cre vs. VGAT-Cre, DAT-Cre vs. VGLUT2-Cre, and VGAT-Cre vs. VGLUT2-Cre). Size factors are estimated and passed as offset terms in the procedure implemented in the DESeq package available for the R statistical programming language as follows: given cell count kij for sample j (j = 1, ..., m) on class i (here, class is synonymous with area / subarea / subregion), the size factor sj for sample j is estimated as

$$\widehat{s_j} = \underset{i}{median} \frac{k_{ij}}{\left(\prod_{v=1}^{m} k_{iv}\right)^{1/m}}$$

We reported the pairwise comparisons computed with these size factors. All p-values were adjusted using the Benjamini-Hochberg method to maintain a family-wise false discovery rate of 5%. See Tables S1 to S6.

Supplemental References

Backman, C.M., Malik, N., Zhang, Y., Shan, L., Grinberg, A., Hoffer, B.J., Westphal, H., and Tomac, A.C. (2006). Characterization of a mouse strain expressing Cre recombinase from the 3' untranslated region of the dopamine transporter locus. Genesis *44*, 383-390.

Hioki, H., Kameda, H., Nakamura, H., Okunomiya, T., Ohira, K., Nakamura, K., Kuroda, M., Furuta, T., and Kaneko, T. (2007). Efficient gene transduction of neurons by lentivirus with enhanced neuron-specific promoters. Gene Ther *14*, 872-882.

Love, M.I., Huber, W., and Anders, S. (2014). Moderated estimation of fold change and dispersion for RNA-seq data with DESeq2. Genome Biol *15*, 550.

Osakada, F., and Callaway, E.M. (2013). Design and generation of recombinant rabies virus vectors. Nat Protoc *8*, 1583-1601.

Osakada, F., Mori, T., Cetin, A.H., Marshel, J.H., Virgen, B., and Callaway, E.M. (2011). New rabies virus variants for monitoring and manipulating activity and gene expression in defined neural circuits. Neuron *71*, 617-631.
Tang, W., Ehrlich, I., Wolff, S.B., Michalski, A.M., Wolfl, S., Hasan, M.T., Luthi, A., and Sprengel, R. (2009). Faithful expression of multiple proteins via 2A-peptide self-processing: a versatile and reliable method for manipulating brain circuits. J Neurosci *29*, 8621-8629.
Vong, L., Ye, C., Yang, Z., Choi, B., Chua, S., Jr., and Lowell, B.B. (2011). Leptin action on GABAergic neurons prevents obesity and reduces inhibitory tone to POMC neurons. Neuron *71*, 142-154.